ACTIVE SUPPRESSION OF AIRCRAFT FLUTTER

H. Hönlinger and A. Lotze
Messerschmitt-Bölkow-Blohm GmbH.
Airplane Division
Postfach 801160, 8 München 80

Abstract

The paper describes design and flight testing of active control systems which are able to suppress store vibrations and flutter as well.

As a first step of development a flutter suppression system is presented which uses additional control surfaces (vanes) mounted on the external stores itself. These control surfaces generate unsteady aerodynamic forces which counteract the motion of the stores.

This system was flight tested on a FIAT G91/T3 and was found to be very effective. It was shown that the system could stabilize an unstable aircraft for a high speed increment above the flutter speed.

This system could also be used as a mode excitation method for improved flight flutter testing for airplanes with wing mounted stores.

The second control system presented in this paper uses the already existing control surfaces of the aircraft to suppress wing store flutter. This system will be flight tested on a F-4F Phantom.

The design of the system will be explained and the optimal control law applied will be discussed.

1. Introduction

During the life time of high performance combat aircraft a large number of new external stores will be developed which must be carried for tactical reasons. Most of these new stores will be accomodated within the already flutter cleared range of weights and radii of gyration of existing stores. Some of these wing mounted stores or store combinations may cause dangerous flutter instabilities within the operational flight envelope. This results in extensive and costly store clearance programs.

The classical means of preventing flutter such as stiffness increase or mass balance are very expensive during service life and also penalize the aircraft's performance. Because of the wide range of different stores and store combinations mounted on the wing pylons, the only suitable means of preventing flutter is limiting the speed.

Many contemporary fighter attack aircraft have flutter restrictions in the range of Ma = 0.7 to Ma = 1.0 at sea level. For large and unconvential stores flutter occurs even at Ma = 0.4 S.L.

In some cases (especially asymmetric store combinations) flutter was not actually encountered; low damping, however, limited the performance of the aircraft.

Based on the growth patterns of aircraft/weapon systems of the past, store flutter limits on advanced aircraft appear inevitable and within the same speed range as they are found today unless improved flutter suppression techniques are defined. It is also believed that the increased use of composite materials will not solve all these wing store flutter problems.

Active flutter suppression is therefore a possible and promising solution.

After a successful application of active flutter suppression on wing store and empennage flutter problems [1 , 2 , 3] in wind tunnels an extension of this technology to a full scale airplane was considered to be rewarding. The effort was focused on the flight test of a wing/store flutter suppression system (FSS).

Objective of these studies were:

- Test of a FSS with store mounted additional vanes.
- Test of a FSS using already existing control surfaces (ailerons) and optimal control laws.
- Provide first flight experience with FSS on external stores.
- Substantiate and demonstrate a new method for flight flutter testing wing mounted stores by use of the FSS (Automatic Mode Excitation System AMES).

This work was carried out under the ZTL research contract for the German Ministry of Defense by the MBB Structural Dynamics Group. The flight test was performed by BWB-LG IV-8 (Bundesamt für Wehrtechnik und Beschaffung) und E-61 (Erprobungsstelle 61 der Bundeswehr) at the German Air Force Test Centre at Manching.

2. Design of the Wing Store Flutter Suppression System using Store mounted Vanes

For the first flight test program with the G91 as flying test bed a single FSS with store mounted vanes to generate the aerodynamic damping forces was chosen which was already tested in the windtunnel. The small vanes on the forward part of the stores don't influence the airplanes steady and unsteady aerodynamic derivativas and can be easily analyzed. Such a system is very apt for a first basic in flight studies.

2.1 Selected Store Configuration

The G91/T3 is flutter free within its flight envelope when carrying its external store inventory. Therefore trend studies were performed to evaluate a critical store configuration which can be simulated by a ballasted 520 ltr. tank (flutter tank). Fig. 1 shows the flutter calculation for the finally selected critical tank configuration.

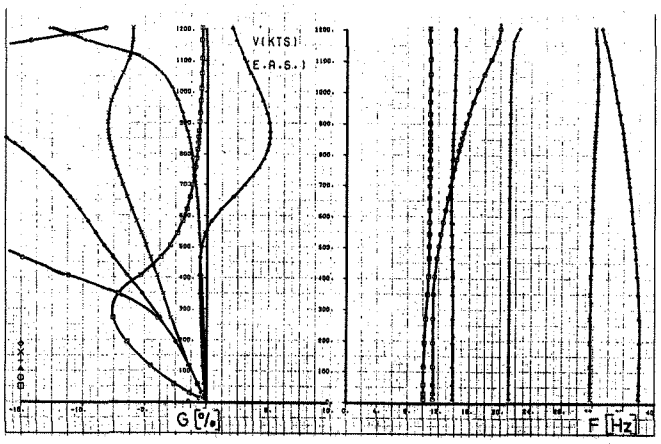

FIG. 1 FLUTTER SPEED VERSUS DAMPING AND FREQUENCY

Two modes, shown in Fig. 2, wing bending at 11.39 Hz and store pitch with wing torsion at 14.15 Hz are causing the flutter case which we intended to suppress.

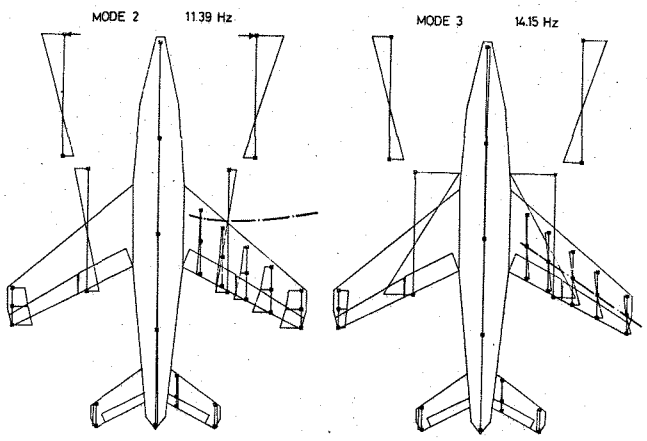

FIG. 2 VIBRATION MODE SHAPES

2.2 Control System

The damping of vibration or flutter modes of wing mounted stores by oscillating vanes creating aerodynamic forces was tested in the wind tunnel to be a very effective way and should now be applied on an airplane. The block diagram in Fig. 3 shows the control loop of the airplane with the FSS and the control law applied.

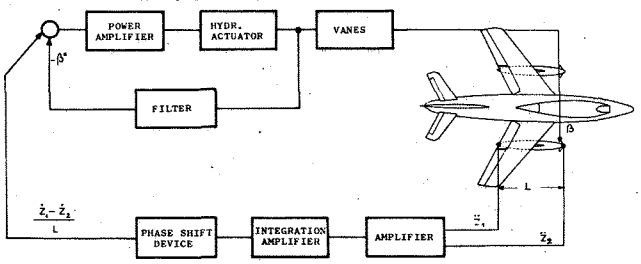

FIG. 3 FLUTTER SUPPRESSION SYSTEM BLOCK DIAGRAM AND CONTROL LAW

This is the concept of a speed proportional damper which introduces selective damping into the flutter mode.

The control signal is produced by two accelerometers located in the forward and rear part of the flutter tank. This signals were added and integrated to give the pitch angle velocity of the flutter store which is used as input signal to the hydraulic actuators driving small vanes attached at the forward part of the store. The vanes oscillate in such a way that the generated airforces counteract the pitch motion of the store like a velocity proportional damper. For optimization of the phase between control signal and angle of attack of the vanes a manual phase shift device was provided in the control loop.

2.3 Analysis of the Vane Control System

An analysis of the airplane with vane control-system was carried out using classical control theory (Root Locus and Nyquist Plot). This analysis predicted that the system could be applied successfully. An explanation of the Nyquist criteria used is shown in Fig. 4.

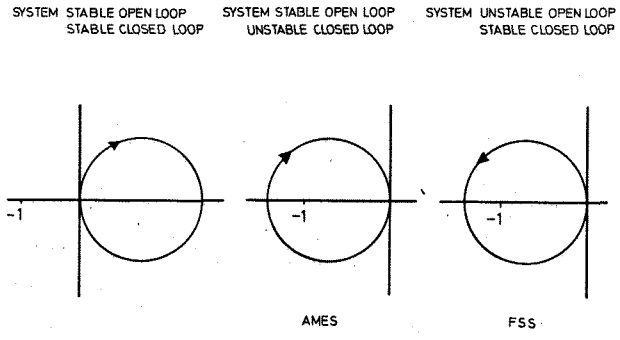

FIG. 4 NYQUIST STABILITY CRITERIA

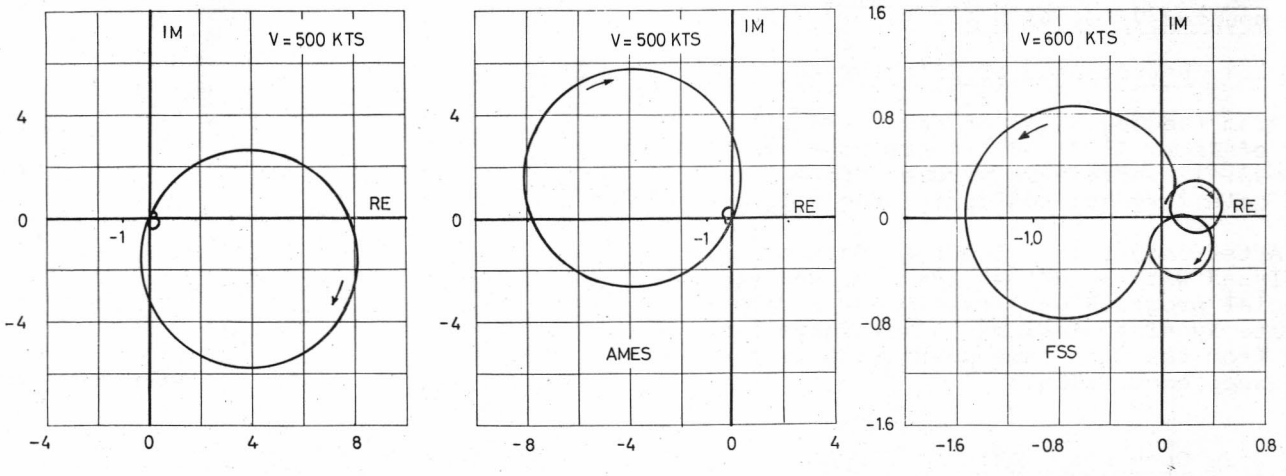

FIG. 5 NYQUIST DIAGRAM FOR THE FLUTTER SUPPRESSION (FSS) AND MODE EXCITATION SYSTEM (AMES)

In Fig. 5 the Nyquist diagram for v = 500 kts for the airplane with FSS is depicted. It shows that the mode to be controlled is stable. With the automatic mode excitation system (AMES) this mode becomes unstable (by means of an artificial instability caused by the control system). For v = 600 kts the system is fluttering and becomes stable only with the FSS.

2.4 Technical Realization of the FSS

As mentioned before the FSS had to be implemented into the two ballasted 520 ltr tanks of the G91. For the sake of redundancy one tank on each wing was installed. Each tank worked independently and only needed electrical power from the aircraft.

Fig. 6 shows a sketch of the installation of the FSS in the 520 ltr. tank. A frame was installed in the forward part of the tank to carry the vanes, the electrohydraulic power package and control electronics. The ballast weight was clamped in the centre part of the tank.

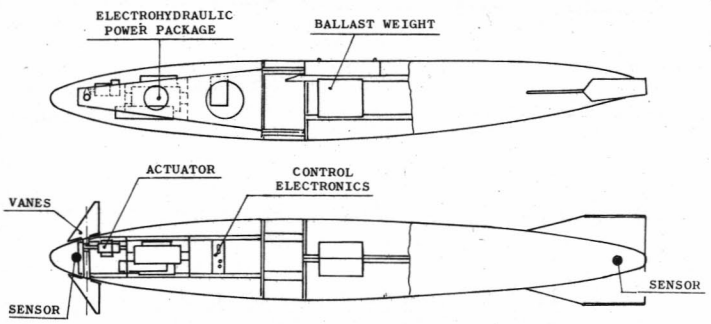

FIG. 6 EXTERNAL TANK WITH FSS (FLUTTER TANK)

The vanes were designed for transsonic flow (anlge of leading edge 30°, axis of rotation at 35 % root chord).

Special fast vane actuators with a mechanical fixing device were developed. The max. torgue the actuators produce is 2700 Ncm. The max. possible angle of attack of the vanes is ± 10°. The weight of the whole FSS in this test status is approx. 21 kg.

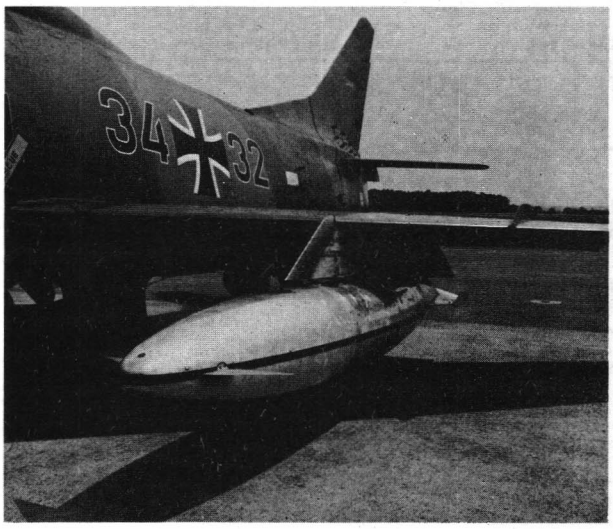

FIG. 7 THE FLUTTER TANK WITH THE FSS MOUNTED ON THE AIRCRAFT

Fig. 7 shows the flutter tank and the vanes on the aircraft.

3. Flight Test of the FSS with Store mounted Vanes on G91

3.1 Performance of Flight Test

From the beginning of Nov. 1976 till end of Febr. 1977 18 flights were performed. 17 parameters were monitored at the telemetry station during the flights.

After each flight the test data were analyzed with an HP 5451 Fourier Analyzer. Special programs were developed to calculate Nyquist diagrams and evaluate damping from the open loop tests with frequency sweep excitation.

3.2 Open Loop Tests in Flight

In order to check the stability and to optimize the phase of the FSS open loop tests in flight at various airspeeds were performed at the beginning of the flight test. Frequency sweeps were fed into the control system. The frequency increased according to a logarithmic law from 5 Hz to 25 Hz and then decreased to 5 Hz within 120 seconds.

Fig. 8 shows the response of the flutter tank to the frequency sweep excitation through the vanes. A good excitation of the flutter mode can be seen.

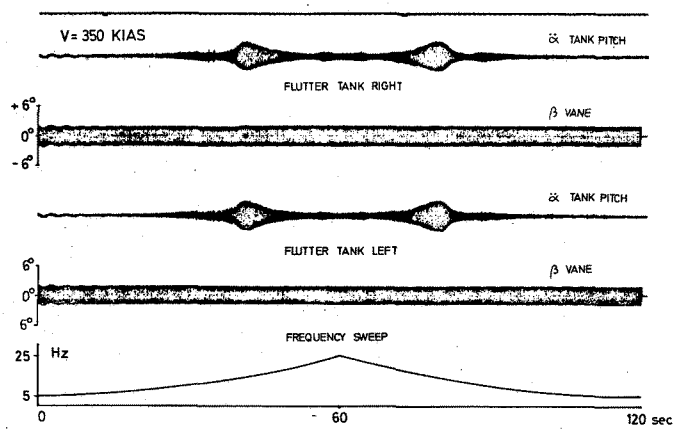

FIG. 8 TIME HISTORY OF FREQUENCY SWEEP EXCITATION (OPEN LOOP)

In Fig. 9 two Nyquist diagrams calculated from these frequency sweeps at v = 350 KIAS and v = 450 KIAS are presented. The phase of the flutter mode is not yet optimized. Comparing both plots the phase shift due to the unsteady air forces can be seen too.

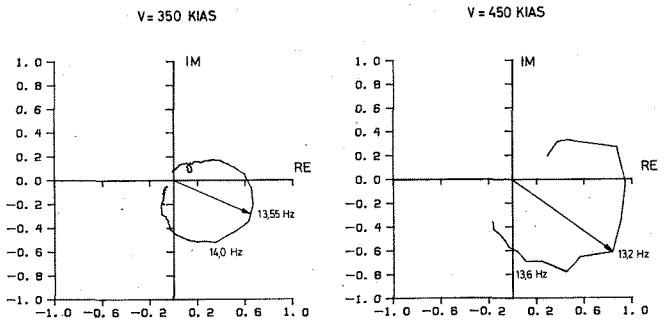

FIG. 9 NYQUIST PLOTS AT V = 350 KIAS AND V = 450 KIAS (OPEN LOOP)

3.3 Closed Loop Tests of the FSS

After having optimized the phase of the flutter mode and having checked the stability of the system within the whole flight range closed loop tests were performed. No valuable test data could be gained by excitation through stick jerks because the frequency content of those excitation signals is too low. The only method to check the closed loop condition is to feed an additional sinusoidal signal (frequency sweep) into the closed loop and analyze the response.

Fig. 10 shows the time history of a closed loop test with electrical frequency sweep input. Comparing Fig. 10 with Fig. 8 one can see that the FSS reduces the vane angle at the frequency of about 14 Hz. The damping coefficient was also evaluated from these tests and is presented later in a summary plot.

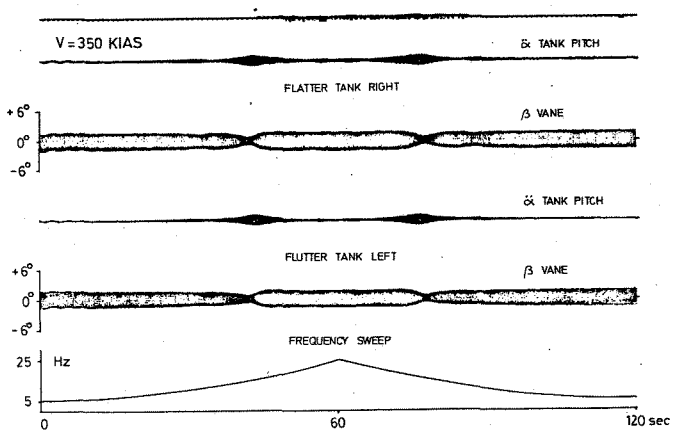

FIG. 10 TIME HISTORY OF FSS RESPONSE DUE TO FREQUENCY SWEEP INPUT

3.4 Tests to Substantiate a New Flight Flutter Test Method for Stores

The aim of this tests was to demonstrate that the modified FSS can be used for a new flight flutter test method as already described in [1].

Fig. 5 shows the principle of the method. If the phase of control signal is shifted 180° the FSS becomes unstable and excites the airplane. This method called Automatic Mode Excitation (AME) has the following outstanding advantages:

- It is automatically tuning the frequency into the store flutter mode and excites it harmonically (provided a suited sensor signal is chosen).
- Switching off the AMES one can easily evaluate the aircraft damping from the logarithmic decrement of the response.
- Combined with the FSS it allows to measure directly the damping trend of the flutter mode above the critical speed.

In comparison with the damping evaluation from frequency sweep response which cannot be done without the help of computers the signals produced by AMES can be analyzed directly by the engineer.

Fig. 11 shows the time history of AMES at various airspeeds. This signals were produced during the flight test. As can be seen high signal to noise ratio allows an evaluation of the damping from the decay at once.

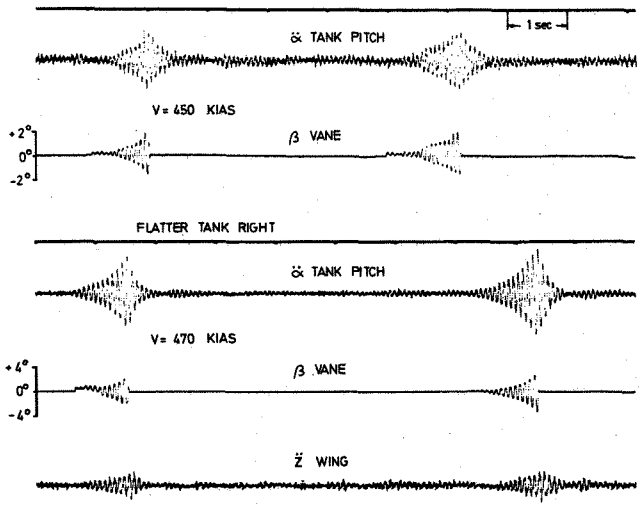

FIG. 11 TIME HISTORY OF AMES V = 450 KIAS AND V = 470 KIAS

The logarithmic increment of the increasing amplitudes shows the excitation of the stable system which can be turned into damping by shifting the phase 180°. The damping evaluated this way has to be added to the damping trend of the flutter mode to get the damping of the stabilized system. This is shown in Fig. 12.

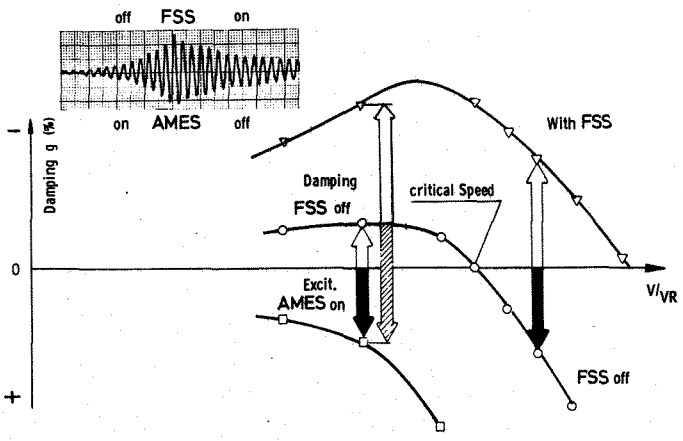

FIG. 12 RELATIONSHIP BETWEEN FSS AND AMES

4. Flight Test Results

4.1 Demonstration of Active Flutter Suppression

During the flight test it was found that the structural damping of the A/C was higher than expected. This increased the flutter speed to a speed which could not be reached anymore. Therefore an artificial flutter case was produced. It was found that the A/C could be driven into flutter at any lower speed using only one system in the AMES mode.

Fig. 13 shows the time history of an artificial flutter case at 300 kts. Using the other system in FSS-mode the instable system became stable.

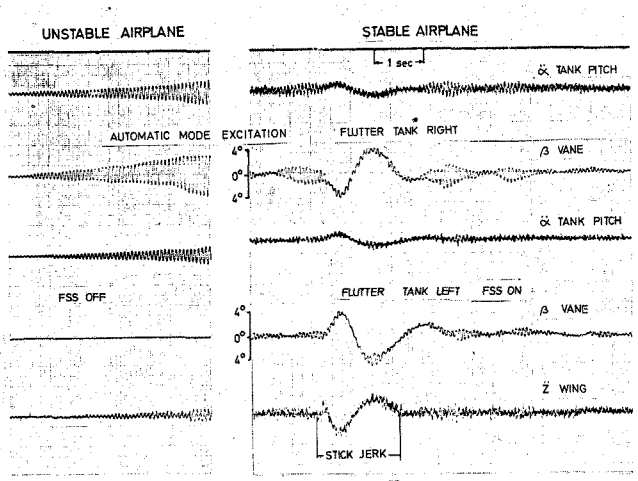

FIG. 13 TIME HISTORY OF STABILIZED SYSTEM AT V = 300 KIAS

The figure demonstrates the response of the unstable and stabilized system. As can be seen, even additional excitation by stick jerks could not destabilize the system.

4.2 Estimated Increase of the Flutter Speed due to FSS

The increase of the real flutter speed could not be demonstrated in flight. In Fig. 14 the increase of the flutter speed is given by extrapolating the measured damping trends. In this picture a medium gain was used to take account of the effects which may occur at high transsonic speeds. Stall of the vanes and saturation conditions of the actuator have to be avoided.

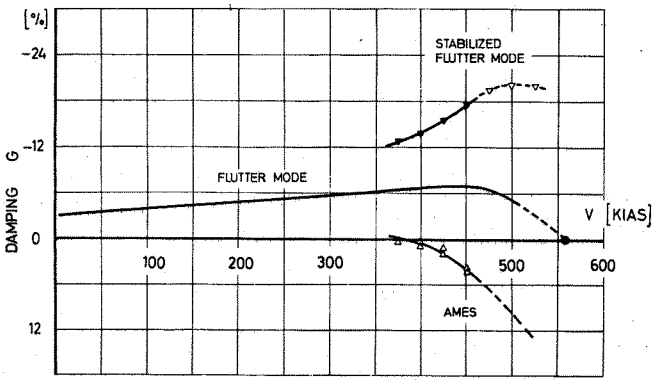

FIG. 14 EFFICIENCY OF FSS

Testing of failure cases:

In a failure case if only one flutter tank works as a damper the efficiency is reduced. In Fig. 15 this effect is shown. If the behaviour of the A/C is symmetrical this effect can be regarded as a gain reduction.

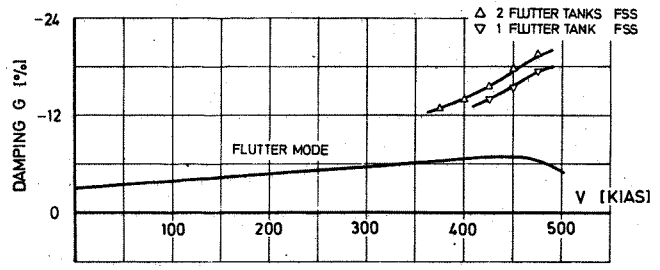

FIG. 15 DAMPING BEHAVIOUR OF FSS IN FAILURE CASE

If one accelerometer of the system fails, the control system uses the vertical acceleration of one sensor as feed back signal. This means theoretically a reduction of the gain of 50 %.

5. Conclusions

It was shown in this first flight test program that a relative simple control system with store mounted vanes can be used for store flutter suppression. This FSS is very effective with relative small vanes which do not change the flight mechanical characteristics of the aircraft.

First flight experience with an AMES was made and the method was found to be promising.

6. Active Flutter Suppression on a F-4F Aircraft with external Stores using already existing Control Surfaces

After the G91 test series with the vane FSS the next logical step was to use already existing control surfaces for the flutter suppression system. A follow on program was started at MBB in 1977. This program is conducted in cooperation with the BWB (Bundesamt für Wehrtechnik und Beschaffung) und the AFFDL (US - Air Force Flight Dynamics Laboratory).

The objective of this program is to develop and flight test a FSS for store flutter which can become a possible candidate for an operational flutter suppression system on any aircraft. Flying test bed for this program is a F-4F aircraft of the German Air Force Test Centre at Manching (Erprobungsstelle 61 der Bundeswehr) equipped for flutter tests.

6.1 Selected Configuration

For this study a wing store configuration on the F-4F with modified stores on the outboard pylon was selected to create a flutter case at about 500 kts.

The results of the flutter calculation for this configuration is shown in Fig. 16. The v-g plot indicates flutter at 465 kts.

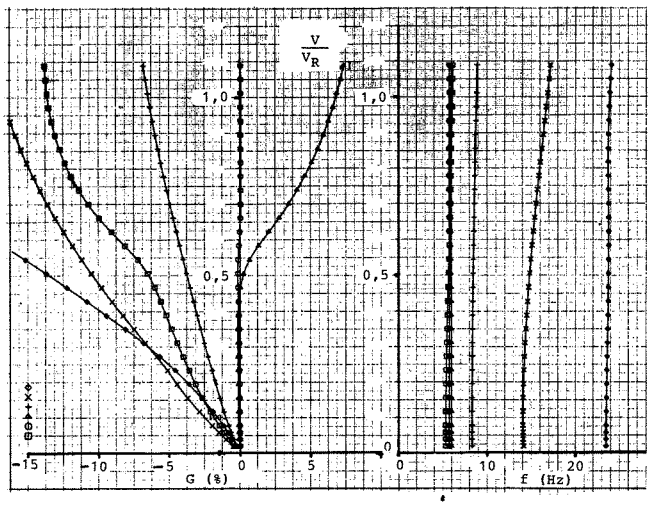

FIG. 16 FLUTTER SPEED VERSUS DAMPING AND FREQUENCY OF THE SELECTED F-4F STORE CONFIGURATION

The flutter is caused by two modes exhibiting large wing bending motion at 5.31 Hz (Mode q_1) and wing torsion store pitch motion at 5.97 Hz (Mode q_2).

6.2 Design of the FSS for the F-4F

As shown in the beginning the vane FSS tested on the G91 could be considered to have no aerodynamic coupling with the aircraft's wing. The system also was independent of the aircraft's control system and hydraulic power supply. Therefore the design of a control law for the FSS had only small constraints (stall of the vanes).

For the design of the F-4F FSS it has to be taken account that the wing aerodynamics are influenced by the aileron deflections. The ailerons are used primerily for flight control purposes. Therefore only small control deflections and actuator power are available for flutter suppression. To match all this constraints much effort was focused on the design of an optimal control law for the FSS.

6.3 The Use of optimal Control Laws for Wing Store Flutter Suppression

Theoretical application of modern control theory for optimal control of an elastic airplane have been reported in several papers [4, 5]. The technical approach for the F-4F program will be described here.

The equations of motion for the forced dynamic response of an aeroelastic system can be written in matrix differential equation form:

$$m_r b_r^2 \begin{bmatrix} M_{qq} & M_{q\beta_0} \\ M_{\beta_0 q} & M_{\beta_0\beta_0} \end{bmatrix} \begin{Bmatrix} \ddot{q} \\ \ddot{\beta}_0 \end{Bmatrix} + \frac{s_R}{k\,v} \left[\omega_r^2 m_r b_r^2 \begin{vmatrix} gK_{qq} & 0 \\ 0 & K''_{\beta_0\beta_0} \end{vmatrix} + \frac{\rho}{2} v^2 F s_R \frac{b_r^2}{s_R^2} \begin{vmatrix} C''_{qq} & C''_{q\beta_0} \\ C''_{\beta_0 q} & C''_{\beta_0\beta_0} \end{vmatrix} \right] \begin{Bmatrix} \dot{q} \\ \dot{\beta}_0 \end{Bmatrix} \tag{1}$$

$$+ \left\{ \omega_r^2 m_r b_r^2 \begin{vmatrix} K_{qq} & 0 \\ 0 & K'_{\beta_0\beta_0} \end{vmatrix} + \frac{\rho}{2} v^2 F s_R \frac{b_r^2}{s_R^2} \begin{vmatrix} C'_{qq} & C'_{q\beta_0} \\ C'_{\beta_0 q} & C'_{\beta_0\beta_0} \end{vmatrix} \right\} \begin{Bmatrix} q \\ \beta_0 \end{Bmatrix} = \{Q(t)\} \tag{1}$$

where m, b_r and ω_r are chosen reference mass, length and frequency and M, K and C are referred to as the generalized mass, stiffness and aerodynamic matrices which are nondimensional. The true airspeed v and the semispan S_R of the reference plane are used to form the reduced frequency $k = (\omega S_R)/V$. F is the area of reference plane and g is the structural damping of the elastic modes. The generalized forces Q are equal to zero for the conventional flutter problem. The generalized coordinate q describes the amplitude of the rigid body modes and the elastic airplane modes including elastic control surface modes for a system with actuators assumed to be rigid, whereas β_0 denotes the rotation of the rigid control surface according to the complex actuator stiffness represented by the impedance function of equation (2).

$$K_{\beta_0\beta_0} = K'_{\beta_0\beta_0} + iK''_{\beta_0\beta_0} \tag{2}$$

For the controlled aircraft the servo-induced control deflection $\Delta\beta$ has to be introduced as an additional degree of freedom for each control surface. The generalized forces Q generated by the servo-induced control deflections $\Delta\beta$ can be described as the right-hand term of equation (1) by

$$\{Q(t)\} = -m_r b_r^2 \begin{Bmatrix} M_{q\Delta\beta} \\ M_{\beta_0\Delta\beta} \end{Bmatrix} \Delta\ddot{\beta} - \frac{\rho}{2} v^2 F s_R \frac{b_r^2}{s_R^2} \frac{s_R}{k\cdot v} \begin{Bmatrix} C''_{q\Delta\beta} \\ C''_{\beta_0\Delta\beta} \end{Bmatrix} \Delta\dot{\beta} - \frac{\rho}{2} v^2 F s_R \frac{b_r^2}{s_R^2} \begin{Bmatrix} C'_{q\Delta\beta} \\ C'_{\beta_0\Delta\beta} \end{Bmatrix} \Delta\beta \tag{3}$$

Assuming normalized rigid control surface modes β_0 and $\Delta\beta$, the rotation of each control surface can be superimposed by

$$\beta = \beta_0 + \Delta\beta \tag{4}$$

For the case described here β is the aileron rotation.

Dividing equation (1) by $m_r \cdot b_r^2 \omega_r^2$, approximating the unsteady aerodynamic forces with a polynominal in $s = i\omega$ at the flutter point

$$(C' + iC'') = a_0 + a_1 s + a_2 s^2 \tag{5}$$

and introducing the actuator transfer function as

$$\frac{\Delta\beta}{x_i} = F_{ACT} = \frac{1}{1 + b_1 s + b_2 s^2} \tag{6}$$

which provides the necessary condition for the added control degree of freedom $\Delta\beta$ then the state-space-description of (1) is as follows:

$$\{\dot{x}\} = [A]\{x\} + [B]\{x_i\} \tag{7}$$

where

$$\{x\} = \begin{Bmatrix} q \\ \beta_0 \\ \Delta\beta \\ \dot{q} \\ \dot{\beta}_0 \\ \Delta\dot{\beta} \end{Bmatrix} = \text{STATE VECTOR} \tag{8}$$

q_1 = wing bending mode

q_2 = wing store pitch mode

β_o = aileron elastic deflection

$\Delta\beta$ = aileron control deflection

Equation (7) can be written by

$$[A] = \begin{vmatrix} 0 & I \\ [S_1]^{-1} \cdot [S_2] & [S_1]^{-1} \cdot [S_3] \end{vmatrix} \qquad (9)$$

using the following matrix notations:

$$[S_1] = \left[\begin{vmatrix} -\frac{1}{\omega_r^2} & & \\ & 1 & \\ & & 1 \end{vmatrix} \begin{vmatrix} M_{qq} & M_{q\beta_0} & M_{q\Delta\beta} \\ M_{\beta_0 q} & M_{\beta_0\beta_0} & M_{\beta_0\Delta\beta} \\ 0 & 0 & \omega_r^2 b_2 \end{vmatrix} + \frac{\rho}{2} v^2 \frac{F}{s_R} \frac{1}{m_r \omega_r^2} \begin{vmatrix} a_{2qq} & a_{2q\beta_0} & a_{2q\Delta\beta} \\ a_{2\beta_0 q} & a_{2\beta_0\beta_0} & a_{2\beta_0\Delta\beta} \\ 0 & 0 & 0 \end{vmatrix} \right]$$

$$[S_2] = \left[\begin{vmatrix} K_{qq} & 0 & 0 \\ 0 & K'_{\beta_0\beta_0} & 0 \\ 0 & 0 & 1 \end{vmatrix} + \frac{\rho}{2} v^2 \frac{F}{s_R} \frac{1}{m_r \omega_r^2} \begin{vmatrix} a_{0qq} & a_{0q\beta_0} & a_{0q\Delta\beta} \\ a_{0\beta_0 q} & a_{0\beta_0\beta_0} & a_{0\beta_0\Delta\beta} \\ 0 & 0 & 0 \end{vmatrix} \right]$$

$$[S_3] = \left[\frac{s_R}{v\,k} \left(\begin{vmatrix} gK_{qq} & 0 & 0 \\ 0 & K''_{\beta_0\beta_0} & 0 \\ 0 & 0 & \frac{v_k}{s_R} b_1 \end{vmatrix} + \frac{\rho}{2} v^2 \frac{F}{s_R} \frac{1}{m_r \omega_r^2} \begin{vmatrix} a_{1qq} & a_{1q\beta_0} & a_{1q\Delta\beta} \\ a_{1\beta_0 q} & a_{1\beta_0\beta_0} & a_{1\beta_0\Delta\beta} \\ 0 & 0 & 0 \end{vmatrix} \right) \right]$$

$$\{B\} = \begin{Bmatrix} 0 \\ 0 \\ 0 \\ [S_1]^{-1} \cdot \begin{bmatrix} 0 \\ 0 \\ 1 \end{bmatrix} \end{Bmatrix}$$

The blockdiagram of this mathematical model of the control system with complete state vector feed back can be seen in Fig. 17.

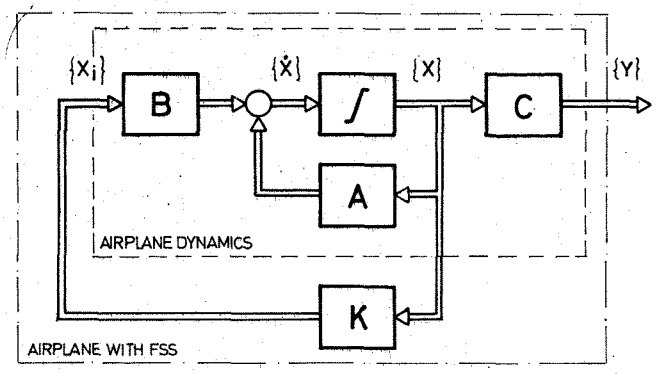

FIG. 17 BLOCK DIAGRAM OF THE CONTROL SYSTEM WITH COMPLETE STATE VECTOR FEEDBACK

To get the optimal control law k_{opt} the quadratic performance criterion is minimized

$$J = \int_0^\infty (\{x\}^T [Q] \{x\} + x_i R x_i)\, dt \qquad (10)$$

Q is a weighting matrix found by trial and error on using a screen together with the computer. R is a scalar, to be selected, because there is only one control surface.

Minimizing (10) leads to the optimal control laws

$$x_i = \{K_{opt}\}^T \{x\} \qquad (11)$$

with

$$\{K_{opt}\}^T = -R^{-1} \{B\}^T [P] \qquad (12)$$

where P is the steady state solution of the Matrix Riccati equation

$$[-\dot{P}] = [P][A] + [A]^T[P] - [P]\{B\}R^{-1}\{B\}^T[P] + [Q] \qquad (13)$$

5.4 Physical Realization of the Control-System with Complete State Vector Feed Back

As we don't have direct access to the state vector x, linear combinations of the sensor outputs can be used to get the state terms

$$\{y\} = [C]\{x\} \qquad (14)$$

where $\{y\}$ is the sensor output and $[C]$ a transformation matrix.

Fig. 18 shows the block diagram for this modified model.

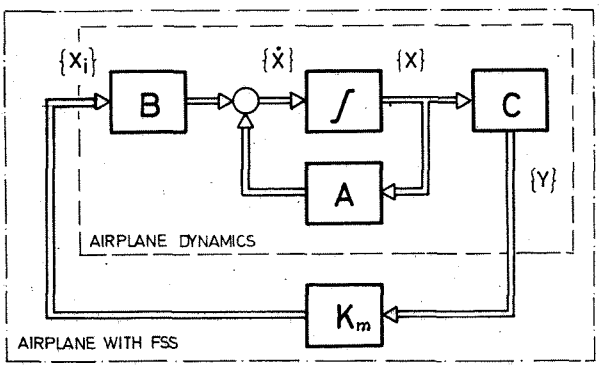

FIG. 18 BLOCK DIAGRAM OF THE CONTROL SYSTEM WITH SENSORS

The control vector $\{K_m\}$ related to the measured vector $\{y\}$ as indicated by Fig.18 can be defined by the inverse transformation matrix $[C^{-1}]$

$$\{K_m\}^T = \{K_{opt}\}^T [C^{-1}] \qquad (15)$$

No problem arises to perform equation (15) if the complete state vector is fed back thus leading to a quadratic form of the transformation matrix C. A band pass filter has to be used to ensure only those modes are fed back which are important for flutter and these modes must be separated by choosing suited sensor locations.

If the number of independent sensor signals is smaller than the size of the state vector, special observers have to be introduced to complete the quadratic form of the transformation matrix.

As mentioned before the F-4F flutter system can be described by two modes

I first wing bending (q_1)

II first wing torsion + store pitch (q_2)

These modes can be measured by two accelerometers on the wing the signals of which will be added and subtracted.

The aileron motion can be described by

$$\frac{m_\beta}{K_\beta} = \beta_0 \qquad (16)$$

where m_β = hinge moment measured by strain gauge

k_β = actuator impedance function

Possible sensor locations on the F-4F for this FSS are given in Fig. 19

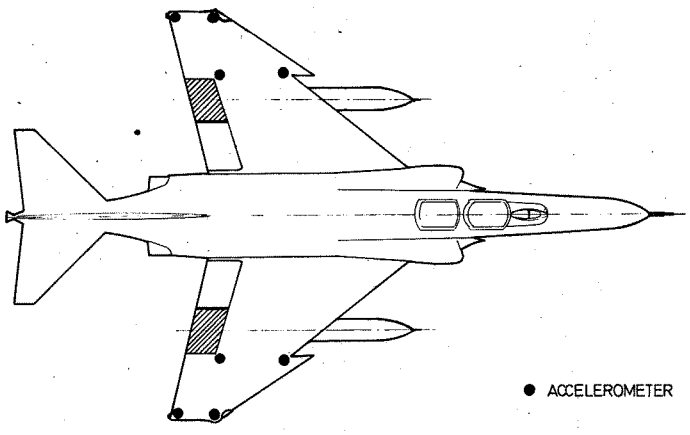

FIG. 19 SENSOR LOCATIONS FOR THE FSS ON THE F-4F

6.4 Results of the Optimization Procedure

For the selected wing store flutter case different control laws were investigated and optimized by variation of the weighting matrix Q and the scalar R of equation (10). The design speed was 600 KEAS representing the flutter situation 35 kts above the flutter speed if 1 % g structural damping is considered. During the optimization procedure it was found that the state terms β_0, $\dot{\beta}_0$, $\Delta\beta$, $\Delta\dot{\beta}$, related to the aileron deflections can be neglected. Therefore the control vector of the FSS presented in Fig. 20 is compound only by the vector product of the state terms which refer to the two modes important for the store flutter case.

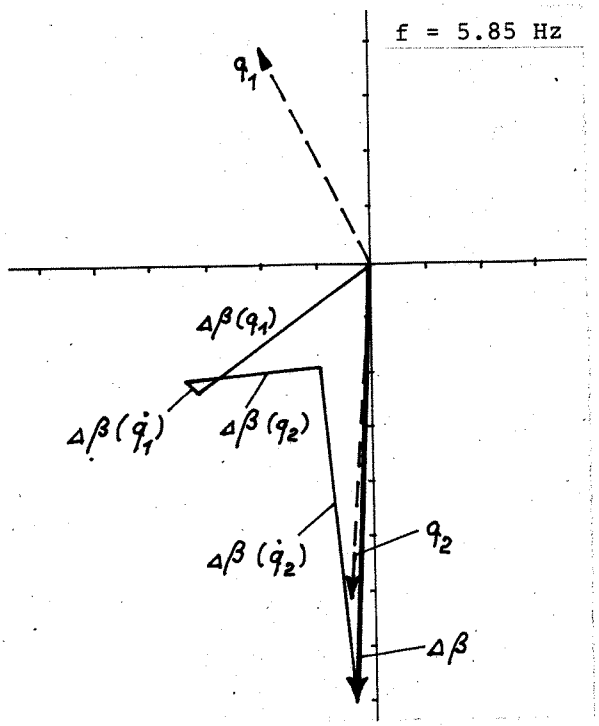

FIG. 20 VECTOR DIAGRAM OF THE CONTROL LAW

Demonstrating an optimized solution for the control law Fig. 20 shows the components of the controlled aileron deflection due to a sinusoidal input at a frequency of the flutter mode. The diagram indicates that the influence of the optimized control system is concentrated on the wing torsion - store pitch mode. It also shows for this flutter case, considering available actuator performance and control surface area, it is more favourable to change the aerodynamic stiffness of the flutter mode rather than to introduce additional damping into this mode.

The efficiency of the control system is demonstrated by the time histories in Fig. 21.

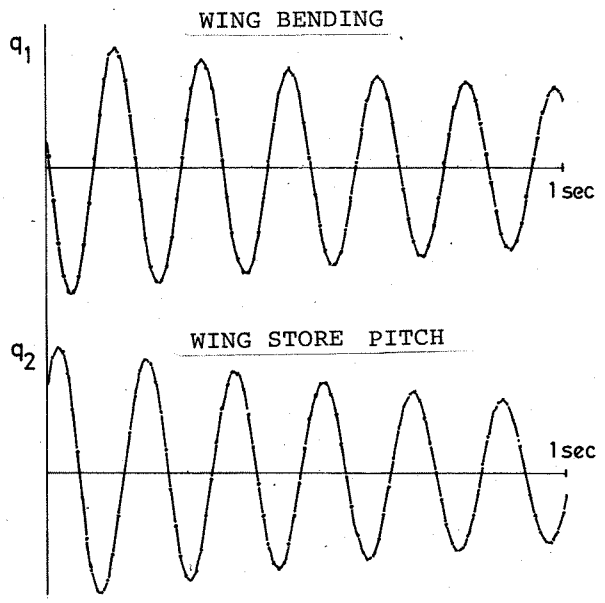

FIG. 21 WING BENDING AND STORE PITCH RESPONSE OF THE STABILIZED AIRCRAFT DUE TO A STEP IMPULS INPUT AT V = 600 KTS

The figure shows the response of the wing bending and wing store pitch mode, which both contribute to the flutter mode, to a step impuls input. The airspeed is about 35 kts above the nominal flutter speed. Both response curves exhibit a damping of approximately 3 % g which proves the achievement in flutter margin is sufficient, considering the damping level usually reached for store flutter modes.

Fig. 22 shows the Nyquist-Diagram of the stabilized F-4F with critical store configuration at v = 600 KEAS.

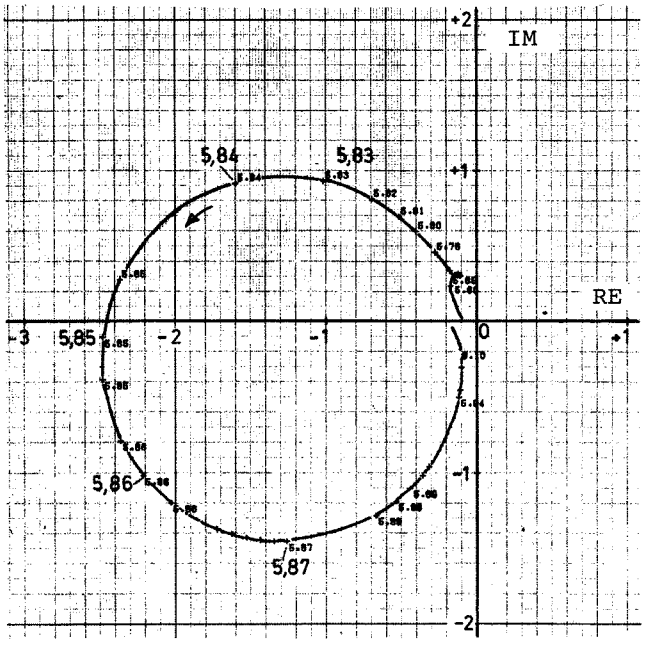

FIG. 22 NYQUIST DIAGRAM OF THE STABILIZED F-4F WITH CRITICAL STORE CONFIGURATION AT V = 600 KEAS

The open loop characteristic of the controlled system proves that the requirements, asking for a stability margin of 6 db and a phase margin of 60 degree are fulfilled.

6.5 Technical Realization of the FSS on the F-4F Aircraft

The flying test bed for the FSS is a F-4F aircraft already used and equipped for flight flutter testing with an aileron excitation system. Therefore only small modifications on the aircraft were necessary to implement the FSS hardware.

To allow an extensive flight testing, the control electronics were designed in a way that 8 modes of operation of the system are possible. These modes are open- and closed loop mode, automatic excitation mode and combinations of these 3 modes.

All modes can be started and cut off by the pilot pressing the trigger button on the stick.

6.6 Safety Installations

To avoid hazardous situations during flight test the same safety installations for the FSS were provided than already used for the G 91 program. Additionally however flutter stop devices were installed into the dummy stores used for flight test. The stores are equipped with movable trimm weights to create mass conditions of the store with a flutter speed around 550 KEAS. In a failure case the trimm weights can be quickly shifted into a "safe" position and stop the flutter by changing the radius of gyration of the store.

6.7 Status of the Flight Test Program

All wing and hardware installations on the aircraft are finished and the checkout of the system is now beginning. After the structural coupling tests of the system flight testing will start in November 1978.

REFERENCES

1 HAIDL, G.; LOTZE, A.; SENSBURG, O.
Active Flutter Suppression on Wings with External Stores
AGARDograph No. 175

2 SENSBURG, O.; HÖNLINGER, H.; KÜHN, M.
Active Control of Empennage Flutter
40th SMP Meeting of AGARD, Brussels/Belgium, 13-18 April 1975

3 HÖNLINGER, H.
Active Flutter Suppression on an Airplane with Wing mounted External Stores
44th SMP Meeting of AGARD, Lisbon/Portugal, 17-22 April, 1977

4 DRESSLER, W.
Control of an Elastic Aircraft using optimal Control Laws
AGARD-CP-157

5 TURNER, M.R.
Active Flutter Suppression
AGARD-CP-175

6 TRIPLETT, W.E.
A Feasibility Study of active Wing/Store Flutter Control
Journal of Aircraft, June 1972

7 TRIPLETT, W.E.; KAPPUS, H.P.F.; LANDY, R.J.
Active Flutter Control
11th AIAA Meeting, Washington, D.C., January 1973